Table VI. Summary of Kinetic Data of the Reactions of Monomeric Ti(IV) Complexes with H_2O_2[a]

complex	k, M^{-1} s^{-1}	T, °C	$\Delta H^{\ddagger}$, kcal mol^{-1}	$\Delta S^{\ddagger}$, cal K^{-1} mol^{-1}
Ti(dipic)	86	15	11.0 ± 0.3	−11.5 ± 1.1
	164	25		
	320	35		
Ti(IDA)	99	15	9.9 ± 0.4	−15 ± 1.2
	176	25		
	326	35		
Ti(NTA)	87	15	10.4 ± 0.3	−13.5 ± 1.0
	170	25		
	302	35		
TiO^{2+} + NCS^- [b]	2.2×10^3	25	11.7	−4.0
TiO^{2+} + HF[b]	1.86×10^3	25	10.6	−8.0

[a] $[H^+]$ = 0.05–1.0 M; I = 1.0 M ($LiClO_4$). [b] Reference 19 (I = 0.50 M).

be present which undergo substitution reactions with H_2O_2. At pH >2 the cyclic tetrameric anion $\{[TiO(NTA)]_4\}^{4-}$ becomes the predominant species in solution which does not have labile coordinated aqua ligands. Therefore, this anion does not react with H_2O_2 (or only very slowly). Only a protonated and/or open-chained tetrameric species reacts rapidly with H_2O_2 ($[H^+]$ = 0.01–0.001 M). The breakdown of the tetrameric structure at $[H^+] > 0.01$ M results in a decrease of rate. Because of the complexity of the equilibria involved, the uncertainty regarding the precise structures of reacting species, and the poor quality of the kinetic runs at pH >1.5, we refrained from studying this pH effect in a more quantitative fashion.

Discussion

It is now well established that titanium(IV) complexes containing a true titanyl moiety, Ti=O, are rarely found[17] in solution or in the solid state. Polymeric species with μ-oxo bridges, Ti–O–Ti, apparently prevail. The absence of strong absorbances in the infrared spectra (800–1050 cm^{-1}, ν(Ti=O) stretching frequency) of our complexes and the X-ray investigation of $Cs_4\{[TiO(NTA)]_4\}\cdot 6H_2O$ revealing a tetrameric anion keep in line with this observation. On the other hand, convincing evidence has been presented that the titanium(IV) aquo ion in aqueous perchloric acid is TiO^{2+}.[19,22] An I_d mechanism for 1:1 formation reactions of TiO^{2+} with NCS^-, HF, and pyrophosphate has been proposed.

From our kinetic experiments we conclude that in perchloric acid media, $[H^+]$ = 0.05–1.0 M, monomeric species of $[Ti(dipic)(OH_2)_3]^{2+}$, $[Ti(IDA)(OH_2)_3]^{2+}$, and $[Ti(NTA)(OH_2)_2]^+$, respectively, are present. The good solubility and the Raman spectra indicate the absence of neutral complexes with a Ti=O group. The reactions of these species with H_2O_2 are not dependent on the hydrogen ion concentration. Values of the respective second-order rate constants (Table VI) fall within a narrow range, and the activation parameters are very similar. They agree well with values obtained for the 1:1 complexing of the TiO^{2+} aquo ion with NCS^- and HF.[19] In addition, the rate constant k_0 = 120 M^{-1} s^{-1} (25 °C, I = 3.0 M) of the $[H^+]$-independent term of the reaction of TiO^{2+} with H_2O_2[10] is also in excellent agreement with the values in Table VI. Therefore, we feel that the present data lend further support to an I_d assignment for the substitution of an aquo ligand coordinated to titanium(IV).

Acknowledgment. Financial support from the Deutsche Forschungsgemeinschaft and the Fonds der chemischen Industrie is gratefully acknowledged.

Registry No. $TiO(dipic)(OH_2)$, 74037-09-5; $TiO(IDA)(OH_2)$, 74037-10-8; $Cs_4\{[TiO(NTA)]_4\}\cdot 6H_2O$, 74050-91-2; TiO(HNTA), 74037-11-9; $[Ti(dipic)(OH_2)_3]^{2+}$, 74037-12-0; $[Ti(IDA)(OH_2)_3]^{2+}$, 74037-13-1; $[Ti(NTA)(OH_2)_2]^+$, 74037-14-2; H_2O_2, 7722-84-1.

Supplementary Material Available: A list of observed and calculated structure factors for $Cs_4\{[TiO(NTA)]_4\}\cdot 6H_2O$ and a list of the anisotropic thermal parameters (25 pages). Ordering information is given on any current masthead page.

(19) Thompson, G. A. K.; Taylor, R. S.; Sykes, A. G. *Inorg. Chem.* **1977**, *16*, 2880.
(20) Sheldrick, G. M., SHELX Crystallographic Calculation Program, University of Göttingen, 1979.
(21) "International Tables for X-Ray Crystallography"; Kynoch Press: Birmingham, England, 1974; Vol. 4.
(22) Ellis, J. D.; Thompson, G. A. K.; Sykes, A. G. *Inorg. Chem.* **1976**, *15*, 3172.

Contribution from the Departments of Chemistry, Tulane University, New Orleans, Louisiana 70118, and The University of Alabama, University, Alabama 35486

Structural, Spectroscopic, and Theoretical Studies of an Exchange-Coupled Manganese(II)–Copper(II) Dimer

JAMES A. PAULSON,[1a] DAVID A. KROST,[1a] GARY L. McPHERSON,*[1a] ROBIN D. ROGERS,[1b] and JERRY L. ATWOOD[1b]

Received November 21, 1979

Crystals of the dimeric complex dichloroaquo(pyridine *N*-oxide)copper(II) which have been doped with manganese(II) contain characterizable quantities of an exchange-coupled Mn(II)–Cu(II) dimer. The EPR spectrum exhibits the fine structure characteristic of a spin quintet (S = 2). The fact that the ground state of the mixed dimer is a quintet indicates that the exchange interactions are antiferromagnetic. The crystal structure of the pure host material has been determined. The complex crystallizes in a triclinic lattice with one centrosymmetric dimer per unit cell. The orientations of the magnetic tensors for the Mn(II)–Cu(II) dimer have been determined and related to the molecular structure. Most of the important features of the spectrum of the mixed dimer can be explained by a set of spin wave functions which are eigenfunctions of the simple isotropic exchange operator ($\mathcal{H} = JS\cdot S'$).

Introduction

Since the early work of Bleaney and Bowers on copper(II) acetate monohydrate, there has been a continuous interest in the spectroscopic and magnetic properties of magnetically coupled dimers. An enormous number of dimeric complexes are now known which contain two interacting paramagnetic centers. Many structural, spectroscopic, and magnetic investigations have been carried out in an effort to elucidate the nature and origin of the magnetic coupling in these complexes.

(1) (a) Tulane University. (b) The University of Alabama.

0020-1669/80/1319-2519$01.00/0

The vast majority of the studies have involved homogeneous dimers where the two interacting paramagnetic centers are identical. Relatively little work on heterogeneous dimer systems has appeared in the literature. In a preliminary communication the EPR spectrum of a heterogeneous dimer containing copper(II) and manganese(II) was reported.[2] The coupled Mn(II)–Cu(II) species was produced by the introduction of a small amount of manganese(II) into crystals of the dimeric complex dichloroaquo(pyridine *N*-oxide)copper(II). The manganese(II) ions substitute for one of the two copper(II) ions in some of the dimeric molecules to give magnetically coupled Mn(II)–Cu(II) systems. Although the concentration of this heterogeneous species in the doped crystals is relatively small, the Mn(II)–Cu(II) dimer is easily observed in the EPR spectra of the doped crystals at liquid-nitrogen temperature. The $[Cu(pyO)Cl_2 \cdot H_2O]_2$ complex behaves as a diamagnetic host lattice at low temperatures, because of the rather strong antiferromagnetic coupling between the copper(II) ions. The spectrum of the Mn(II)–Cu(II) dimer exhibits hyperfine structure because of both the copper and manganese nuclei and indicates that the exchange interaction is antiferromagnetic. The **g** tensor of the system was thought to be unusual since the three principal values are all measurably smaller than the free-electron value of 2.0023. The *g* values associated with copper(II) complexes are invariably larger than the free-electron value while those associated with high-spin manganese(II) are usually quite close to that of the free electron. This paper presents the results of structural, spectroscopic, and theoretical studies directed toward the characterization of this unusual heterogeneous magnetic dimer. The crystal structure of the $[Cu(pyO)Cl_2 \cdot H_2O]_2$ complex has been determined, and the approximate molecular orientations of the magnetic tensors have been obtained. A simple and straightforward theoretical model is developed which accounts for most of the properties of the Mn(II)–Cu(II) dimer, including the *g* values.

Experimental Section

Preparation of the Doped Crystals. The anhydrous pyridine *N*-oxide complex, $[Cu(pyO)Cl_2]_2$, was prepared according to the procedure of Quagliano and co-workers.[3] Methanol rather than ethanol was used as the solvent. Pyridine *N*-oxide complexes of $ZnCl_2$ and $MnCl_2$ were prepared in a similar fashion. Equimolar quantities of the hydrated metal dichloride and pyridine *N*-oxide were dissolved separately in small volumes of methanol. The methanol solutions were then mixed and allowed to stand for 1 h. During that time the complexes precipitated from solution. Neither the zinc nor manganese complex was characterized in detail. Mixtures of the copper complex and either the zinc or the manganese complex (about 3 to 1 in favor of copper) were dissolved in methanol containing approximately 25% water. Slow evaporation of these solutions yielded large single crystals of the hydrated complex $[Cu(pyO)Cl_2 \cdot H_2O]_2$, which contained small concentrations of either Mn(II) or Zn(II). Most of these crystals grew as six-sided plates where the principal face of the plate corresponded to the *ac* plane.

EPR Spectra. The EPR spectra were recorded at X-band frequency on a Varian E-3 spectrometer and at Q-band frequency on a Varian E-12 spectrometer. Both instruments used 100-kHz field modulation. The field dial of the E-12 was calibrated with a Spectromagnetic Industries gaussmeter. Microwave frequencies were determined by measuring the resonance field of polycrystalline DPPH ($g = 2.0036$).

X-ray Data Collection and Structure Determination. Crystals of undoped $[Cu(pyO)Cl_2 \cdot H_2O]_2$ were grown by slow evaporation of solutions prepared by dissolving the anhydrous copper pyridine *N*-oxide complex in aqueous methanol (~25% H_2O). Single crystals of the compound were sealed in thin-walled glass capillaries prior to X-ray examination. Final lattice parameters as determined from a least-squares refinement of the angular settings of 15 reflections ($2\theta > 20°$) accurately centered on an Enraf-Nonius CAD-4 diffractometer are given in Table I.

Table I. Crystal Data

mol formula	$Cu_2Cl_4O_4N_2C_{10}H_{14}$	cell vol, Å^3	433.7
mol wt	495.1	linear abs coeff, cm^{-1}	31.7
cell constants[a]		space group	$P\bar{1}$
a, Å	5.912 (2)	molecules/unit cell	1
b, Å	7.973 (3)	max cryst dimens, mm	0.40 × 0.32 × 0.42
c, Å	9.462 (3)	calcd density, g/cm^{-3}	1.90
α, deg	81.25 (3)	measd density, g/cm^{-3}	1.87
β, deg	81.06 (3)		
γ, deg	83.66 (2)		

[a] Mo Kα radiation, λ = 0.710 69 Å. The ambient temperature is 23 ± 1 °C.

Data were collected on the diffractometer with graphite-crystal monochromated molybdenum radiation. The diffracted intensities were collected by the ω–2θ scan technique with a takeoff angle of 3.0°. The scan rate was variable and was determined by a fast (20°/min) prescan. Calculated speeds based on the net intensity gathered in the prescan ranged from 7 to 0.3°/min. Moving-crystal moving-counter backgrounds were collected for 25% of the total scan width at each end of the scan range. For each intensity the scan width was determined by

$$\text{scan range} = A + B \tan\theta$$

where $A = 0.80°$ and $B = 0.20°$. Aperture settings were determined in a like manner with $A = 4$ mm and $B = 2.11$ mm. Other diffractometer parameters and a method of estimation of the standard deviations have been described previously.[4] As a check on the stability of the instrument and crystal, two reflections, (040) and (005), were measured after every 50 reflections; no significant variation was noted. One independent hemisphere of data was measured out to $2\theta = 50°$; a slow scan was performed on a total of 1325 unique reflections. Since these data were scanned at a speed which would yield a net count of 4000, the calculated standard deviations were all fairly equal. No reflection was subject to a slow scan unless a net count of 25 was obtained in the prescan. On the basis of these considerations, the data set of 1325 reflections (used in the subsequent structure determination and refinement) was considered observed and consisted in the main of those for which $I \geq 3\sigma(I)$. The intensities were corrected for Lorentz and polarization effects but not for absorption ($\mu = 31.7$ cm^{-1}).

Full-matrix, least-squares refinement was carried out in which the function $w(|F_o| - |F_c|)^2$ was minimized. No corrections were made for extinction. Atomic scattering factors for Cu, Cl, N, and C were taken from Cromer and Waber;[5] those for H were from ref 6. The scattering for Cu was corrected for the real and imaginary components of anomalous dispersion by using the values of Cromer and Liberman.[7] All the calculations were carried out by using standard crystallographic computer programs.[8]

The space group was determined to be $P\bar{1}$. The existence of 1 molecule per unit cell required the molecule to reside on a crystallographic center of inversion. Inspection of a Patterson map revealed the position of the copper atom. Difference Fourier maps using the copper position revealed all nonhydrogen atoms. Several cycles of least-squares refinement of the positional and isotropic thermal parameters of the nonhydrogen atoms afforded a reliability index of $R_1 = \sum(|F_o| - |F_c|)/\sum|F_o| = 0.092$. Conversion to anisotropic thermal parameters and further refinement gave $R_1 = 0.051$. Those positions of the hydrogen atoms that could be calculated were refined for two cycles at a damping factor of 0.2. The remaining two hydrogen atom positions were determined from a difference Fourier map and refined

(2) D. A. Krost and G. L. McPherson, *J. Am. Chem. Soc.*, **100**, 989 (1978).
(3) J. V. Quagliano, J. Fujita, G. Franz, D. J. Phillips, J. A. Walmsley, and S. Y. Tyree, *J. Am. Chem. Soc.*, **83**, 3770 (1961).
(4) J. L. Atwood and K. D. Smith, *J. Am. Chem. Soc.*, **95**, 1488 (1973).
(5) D. T. Cromer and J. T. Waber, *Acta Crystallogr.*, **18**, 104 (1965).
(6) "International Tables for X-Ray Crystallography", Vol. III, Kynoch Press, Birmingham, England, 1962, p 205.
(7) D. T. Cromer and D. Liberman, *J. Chem. Phys.*, **53**, 189 (1970).
(8) Crystallographic programs used on a UNIVAC 1110 include ALFF (Fourier synthesis, by C. R. Hubbard, C. O. Quicksall, and R. A. Jacobson), ORFLS (structure factor calculation and least-squares refinement, by W. R. Busing, K. O. Martin, and H. A. Levy), ORFFE (distances and angles with esd's, by W. R. Busing, K. O. Maring, and H. A. Levy), and ORTEP (thermal ellipsoid drawings, by C. K. Johnson).

Table II. Final Fractional Coordinates and Anisotropic Thermal Parameters[a]

atom	x/a	y/b	z/c	β_{11}	β_{22}	β_{33}	β_{12}	β_{13}	β_{23}
Cu	0.1598 (1)	0.1480 (1)	0.4124 (1)	0.0146 (2)	0.0081 (1)	0.0061 (1)	−0.0048 (1)	0.0015 (1)	−0.0021 (1)
Cl(1)	0.4074 (2)	0.1481 (2)	0.2102 (1)	0.0172 (4)	0.0127 (2)	0.0073 (2)	−0.0030 (2)	0.0030 (2)	−0.0016 (2)
Cl(2)	0.3028 (2)	0.3481 (2)	0.5014 (2)	0.0207 (4)	0.0100 (2)	0.0085 (2)	−0.0071 (2)	−0.0022 (2)	−0.0020 (2)
O(1)	−0.0285 (7)	0.0661 (5)	0.6007 (4)	0.0323 (15)	0.0112 (7)	0.0066 (5)	−0.0094 (8)	0.0048 (7)	−0.0052 (5)
O(2)	−0.1475 (7)	0.3196 (5)	0.3219 (5)	0.0180 (13)	0.0125 (7)	0.0118 (6)	−0.0002 (8)	−0.0015 (7)	−0.0027 (5)
N	−0.0726 (7)	0.1557 (5)	0.7180 (4)	0.0195 (14)	0.0074 (6)	0.0047 (5)	−0.0027 (8)	0.0000 (6)	−0.0024 (4)
C(1)	0.0750 (10)	0.1308 (8)	0.8120 (7)	0.0212 (20)	0.0139 (11)	0.0095 (8)	−0.0024 (12)	−0.0048 (10)	0.0014 (7)
C(2)	0.0322 (14)	0.2239 (10)	0.9273 (7)	0.0441 (32)	0.0246 (17)	0.0067 (8)	−0.0179 (20)	−0.0075 (12)	0.0023 (9)
C(3)	−0.1585 (16)	0.3362 (10)	0.9412 (8)	0.0509 (35)	0.0180 (14)	0.0086 (9)	−0.0127 (18)	0.0058 (14)	−0.0061 (9)
C(4)	−0.3024 (13)	0.3580 (9)	0.8401 (8)	0.0344 (27)	0.0145 (13)	0.0133 (10)	0.0013 (14)	0.0067 (14)	−0.0053 (9)
C(5)	−0.2561 (10)	0.2656 (7)	0.7274 (6)	0.0211 (19)	0.0113 (10)	0.0083 (7)	−0.0001 (11)	−0.0017 (9)	−0.0003 (7)

atom	x	y	z	B, Å²	atom	x	y	z	B, Å²
H(C1)	0.200	0.060	0.793	5.2	H(C5)	−0.355	0.276	0.654	3.9
H(C2)	0.135	0.210	1.001	6.4	H(1)	−0.202	0.404	0.362	5.3
H(C3)	−0.177	0.386	1.028	7.9	H(2)	−0.304	0.253	0.330	5.3
H(C4)	−0.441	0.431	0.848	4.4					

[a] Anisotropic thermal parameters defined by $\exp[-(\beta_{11}h^2 + \beta_{22}k^2 + \beta_{33}l^2 + 2\beta_{12}hk + 2\beta_{13}hl + 2\beta_{23}kl)]$.

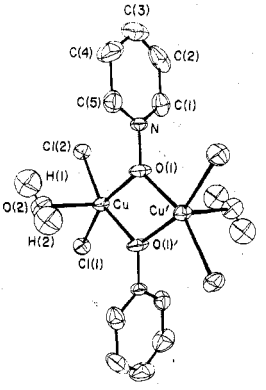

Figure 1. ORTEP drawing of a single dimeric unit in $[Cu(pyO)Cl_2 \cdot H_2O]_2$.

similarly. More cycles of refinement led to final values of $R_1 = 0.036$ and $R_2 = \{\sum w(|F_o| - |F_c|)^2 / \sum (F_o)^2\}^{1/2} = 0.044$. The largest parameter shifts in the final cycle of refinement were less than 0.01 of their estimated standard deviations. A final difference Fourier showed no feature greater than 0.3 e/Å³. The standard deviation of an observation of unit weight was 1.53. Unit weights were used at all stages; no systematic variation of $w(|F_o| - |F_c|)$ vs. $|F_o|$ or $(\sin\theta)/\lambda$ was noted. The final values of the positional and thermal parameters are given in Table II.

Results and Discussion

Structure of $[Cu(pyO)Cl_2 \cdot H_2O]_2$. The diffraction studies show that the dichloroaquo(pyridine *N*-oxide)copper(II) complex is dimeric with bridging *N*-oxide groups. The basic structure is consistent with that initially predicted by Kokoszka and co-workers on the basis of EPR measurements.[9,10] An ORTEP drawing of a single dimeric unit is shown in Figure 1, while selected bond distances and angles are reported in Table III. The basic structure can be described as two distorted square-pyramidal copper(II) complexes joined at a basal edge such that the resulting dimer has inversion symmetry. The water molecules occupy the two apical positions while the oxygen atoms of the *N*-oxide ligands and the chloride ions make up the basal plane. The maximum deviation from the best-fit least-squares plane through the basal atoms is 0.04 Å, and the copper(II) ions are located approximately 0.23 Å out of this plane. The bond from the copper(II) ion to the apical water molecule is parallel (within 3°) to the normal of the least-squares plane. Apparently, the repulsion between

Table III. Bond Lengths (Å) and Bond Angles (Deg)[a]

Cu–Cl(1)	2.221 (1)	N–C(1)	1.319 (7)
Cu–Cl(2)	2.213 (1)	C(1)–C(2)	1.387 (10)
Cu–O(1)	2.007 (4)	C(2)–C(3)	1.363 (12)
Cu–O(1)′	1.979 (4)	C(3)–C(4)	1.355 (11)
Cu–O(2)	2.342 (4)	C(4)–C(5)	1.364 (9)
Cu···Cu′	3.272 (1)	C(5)–N	1.318 (7)
O(1)–N	1.386 (5)	O(2)–H[b]	0.96
Cl(1)–Cu–Cl(2)	97.44 (5)	Cl(2)–Cu–O(1)	93.9 (1)
Cl(1)–Cu–O(1)	161.1 (1)	Cl(2)–Cu–O(1)′	161.2 (1)
Cl(1)–Cu–O(1)′	96.2 (1)	Cl(2)–Cu–O(2)	97.2 (1)
Cl(1)–Cu–O(2)	99.4 (1)	O(1)–Cu–O(1)′	69.7 (2)
O(1)–Cu–O(2)	94.0 (2)	O(1)′–Cu–O(2)	93.2 (2)
Cu–O(1)–Cu	110.3 (2)	Cu′–O(1)–N	125.6 (3)
Cu–O(1)–N	123.9 (3)	C(1)–C(2)–C(3)	119.9 (6)
O(1)–N–C(1)	118.4 (5)	C(2)–C(3)–C(4)	119.4 (6)
O(1)–N–C(5)	118.2 (4)	C(3)–C(4)–C(5)	119.6 (7)
C(1)–N–C(5)	123.4 (5)	C(4)–C(5)–N	119.7 (6)
N–C(1)–C(2)	118.0 (6)	H(1)–O(2)–H(2)	100

[a] Primed atoms related to those in Table II by $(-x, -y, 1-z)$. [b] Average of O(2)–H(1) and O(2)–H(2).

the two copper(II) ions causes the Cu–O(1)–Cu′ bridging angle to open out to 110°, resulting in an internal O(1)–Cu–O(1)′ angle of about 70° which is about 20° smaller than that for an idealized square-pyramidal structure. The bond distances indicate that the apical water molecule is not bound as tightly to the copper(II) ion as are the ligands in the basal plane. This is typical of pentacoordinate copper(II) complexes. In general, the molecular structure of $[Cu(pyO)Cl_2 \cdot H_2O]_2$ is quite comparable to those of other similar amine *N*-oxide bridged copper(II) dimers.[11]

Although the complex is best described as a discrete dimer, there appear to be some weak interdimeric interactions. The diffraction data indicate that the protons of the apical water molecules are hydrogen bonded to the chloride ions of neighboring dimers. The interatomic distances show that H(1) is hydrogen bonded to the Cl(2) of an adjacent dimer while H(2) interacts with the Cl(1) from a second dimer. In both cases the H···Cl distance is approximately 2.5 Å. A weak magnetic coupling between dimers might arise as a result of the hydrogen-bonding interactions; however, such interdimeric coupling should have little impact on the magnetic properties of the material. The magnetic behavior of $[Cu(pyO)Cl_2 \cdot H_2O]_2$ is almost certainly dominated by the rather strong antiferromagnetic intradimeric coupling of the copper(II) ions. Kokoszka and co-workers[9] determined that the singlet–triplet separation was approximately 880 cm^{-1} which is far larger than

(9) G. F. Kokoszka, H. C. Allen, Jr., and G. Gordon, *J. Chem. Phys.*, **46**, 3013 (1967).
(10) G. F. Kokoszka, H. C. Allen, Jr., and G. Gordon, *J. Chem. Phys.*, **46**, 3020 (1967).
(11) W. H. Watson, *Inorg. Chem.*, **8**, 1879 (1969).

would be expected from any type of interdimeric interactions.

When other divalent metal ions are doped into crystals of $[Cu(pyO)Cl_2 \cdot H_2O]_2$, the impurity ions apparently replace one of the two copper(II) ions in some of the complexes to produce mixed metal dimers.[2,9] Although some structural change must accompany the replacement, it is assumed that the spectra of the mixed metal systems can be adequately interpreted in terms of the crystal structure of the pure material.

EPR Spectra of Doped $[Cu(pyO)Cl_2 \cdot H_2O]_2$ Crystals. When a high-spin manganese(II) ion ($S = {}^5/_2$) is exchange coupled to a copper(II) ion ($S = {}^1/_2$), the resulting dimer is characterized by two spin states, a quintet ($\Sigma = 2$) and a septet ($\Sigma = 3$). We have adopted the convention that S refers to the spins of individual ions while Σ refers to the spins of the complete dimeric system. The ordering and relative energies of the two states is determined by the nature and magnitude of the exchange interaction. If the coupling is antiferromagnetic, the quintet will be lower in energy. As previously reported, the EPR spectrum of $[Cu(pyO)Cl_2 \cdot H_2O]_2$ crystals doped with Mn(II) at 77 K exhibits the fine structure characteristic of a system with a total spin of 2. In addition, the hyperfine structure from the copper and manganese nuclei (^{63}Cu and ^{65}Cu, $I = {}^3/_2$; ^{55}Mn, $I = {}^5/_2$) is clearly resolved. There is little doubt that the spectrum arises from the quintet state of an exchange-coupled manganese(II)–copper(II) dimer. No resonances which can be assigned to the septet state are observed, even when the crystals are warmed from 77 to 250 K. Above 250 K the resonances from the thermally populated triplet state of the pure copper(II) dimers begin to obscure the resonances from the mixed dimers which are present in a relatively small concentration. The fact that the only observed resonances arise from the quintet state of the manganese(II)–copper(II) system clearly indicates that the exchange is antiferromagnetic and suggests that the septet state is at least 150 cm^{-1} above the ground-state quintet.

The fact that the triclinic unit cell contains only one dimer is a significant advantage in the analysis of the EPR spectra. Unfortunately, this advantage is partially offset by the low symmetry of the lattice. The absolute orientations of the magnetic axes in a triclinic crystal are difficult to determine accurately with the equipment used in this study. The results reported here represent the average of a number of separate determinations. The spectrum of the mixed dimer is satisfactorily described by an effective spin Hamiltonian which is written for a low symmetry system with a spin of two. This spin Hamiltonian in compact form is

$$\mathcal{H} = \beta H \cdot \bar{g} \cdot \Sigma + D(\hat{\Sigma}_Z^2 - 2) + E(\hat{\Sigma}_X^2 - \hat{\Sigma}_Y^2) + I_c \cdot \bar{A}_c \cdot \Sigma + I_m \cdot \bar{A}_m \cdot \Sigma$$

The first term represents the electron–Zeeman interaction while the next two terms describe the zero-field splitting. The final two terms contain the electron–nuclear hyperfine interactions for the copper and manganese nuclei. For molecules of low symmetry the principal axes of the different magnetic tensors are, in general, not coincident. Rigorously speaking, mixed metal dimers in $[Cu(pyO)Cl_2 \cdot H_2O]_2$ have no symmetry at all. Thus, there is no required relationship between the principal axes of the magnetic tensors and the crystallographic axes.

Since the zero-field splitting is fairly large, the fine structure is the easiest of the spectral features to follow as a function of crystal orientation. It is apparent from the spin Hamiltonian parameters given in Table IV that there is a large rhombic component to the zero-field splitting tensor. Figure 2 shows the spectra observed when the magnetic field is directed along the X and Z axes of the zero-field splitting tensor. In both orientations the four-line fine structure is clearly evident. Along the X axis, the four-line patterns resulting from hyperfine interaction with the copper nucleus (^{63}Cu and ^{65}Cu) can be easily seen superimposed on the six-line manganese hyperfine patterns. When the field is directed along the Y axis of the zero-field splitting tensor, the separation between fine structure components is sufficiently small that the fine and hyperfine structures overlap considerably. The orientation of the axes of the zero-field splitting tensor with respect to the molecular framework of the $[Cu(pyO)Cl_2 \cdot H_2O]_2$ dimer is shown in Figure 3. The Z axis lies within 5° of the least-squares plane defined by the oxygen atoms of the N-oxide ligands and the chloride ions. The other two axes do not appear to be directed along any prominent structural feature. We estimate that the locations of the zero-field splitting axes are correct within 10°.

Table IV. Spin Hamiltonian Parameters[a]

Manganese(II)–Copper(II) Dimer

g values	hyperfine constants, cm^{-1}		zero-field splitting constants, cm^{-1}
	^{55}Mn	^{63}Cu and ^{65}Cu	
$g_x = 1.991$	$A_X = 0.0091$	$A_x < 0.0005$	$D = \pm 0.051$
$g_y = 1.986$	$A_Y = 0.0091$	$A_y < 0.0005$	$E = \pm 0.013$
$g_z = 1.952$	$A_Z = 0.0090$	$A_z = 0.0023$	

Copper(II)–Zinc(II) Dimer

$g_x = 2.056$ $g_y = 2.083$ $g_z = 2.306$

[a] The subscripts x, y, and z refer to the principal axes of the **g** tensor and X, Y, and Z refer to the principal axes of the zero-field tensor. The Cu(II)–Zn(II) g values were taken from ref 10.

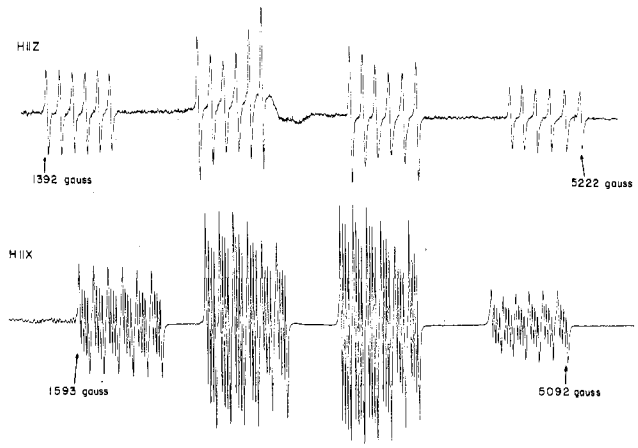

Figure 2. EPR spectra of two crystals of $[Cu(pyO)Cl_2 \cdot H_2O]$ doped with Mn(II) recorded at X-band frequency. In both cases the temperature was 77 K. One crystal (upper trace) was mounted so that the field of the spectrometer was parallel to the Z axis of the zero-field splitting tensor. The second crystal (lower trace) was oriented such that the field was parallel to the X axis of the zero-field splitting tensor.

The **g** tensor of the manganese(II)–copper(II) dimer is noticeably anisotropic; however, the anisotropy is not nearly as large as that observed in ordinary copper(II) complexes. The orientation of the principal axes of the **g** tensor is shown in Figure 4. The orientation is quite different from that of the zero-field splitting tensor. (The X, Y, and Z axes refer to the zero-field splitting while the x, y, and z axes refer to the **g** tensor.) Because the variation of the g value in the xy plane is quite small, the location of the x and y axes are not precise. The location of the z axis, however, should be accurate within 10°. The z axis is very nearly parallel to the bond between the apical water molecule and the copper(II) ion. This direction corresponds closely to the normal of the least-squares plane defined by the six equatorially bonded ligand atoms.

The hyperfine interaction with the copper nucleus is very anisotropic. The Cu coupling constant appears to maximize along the z axis of the **g** tensor. As the plane perpendicular to the z axis is approached, the coupling constant becomes too

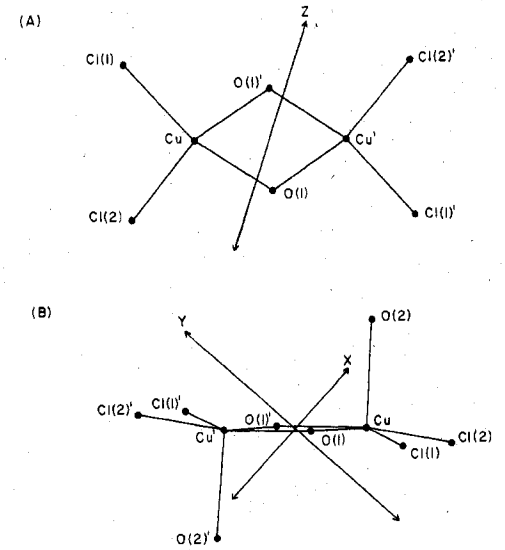

Figure 3. Orientation of the principal axes of the zero-field tensor. Part A is the projection of the Z axis of the zero-field tensor onto the least-squares plane through the six equatorially bonded ligand atoms. The Z axis lies within 5° of this plane. Part B is the projection of the dimer onto the plane defined by X and Y axes of the zero-field tensor.

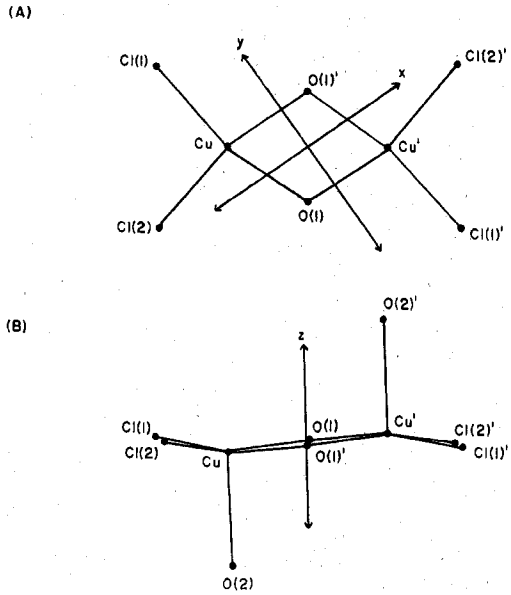

Figure 4. Orientation of the principal axes of the **g** tensor. In part A the x and y axes of the **g** tensor are projected onto the least-squares plane through the six equatorially bonded ligand atoms. These axes lie within 4° of this plane. The x axis is directed roughly along the Cu–O(1)′ bond while the y axis is nearly parallel to the Cu–Cl(1) bond. Part B shows the projection of the z axis of the **g** tensor onto the plane that is perpendicular to the least-squares plane and parallel to the line passing through the copper nuclei. The z axis is approximately parallel to the Cu–O(2) bond and to the normal of the least-squares plane.

small to measure. The collapse of the copper hyperfine structure in this plane is quite evident in the spectrum taken along the Z axis of the zero-field splitting tensor (see Figure 2). In contrast to the copper hyperfine interaction, the hyperfine tensor for the manganese nucleus is essentially isotropic. The Mn coupling constants reported in Table IV are evaluated along the axes of the zero-field splitting tensor.

In order to elucidate the magnetic properties of a single copper(II) ion in the dimeric complex, we prepared and studied crystals of $[Cu(pyO)Cl_2 \cdot H_2O]_2$ doped with divalent zinc. Since zinc(II) is diamagnetic, the mixed dimers behave as monomeric copper(II) complexes. This copper(II)–zinc(II) system has already been characterized in some detail.[10] The primary purpose for our investigation was to locate the axes of the **g** tensor. The orientation of these axes was found to be the same as the orientation of the **g** tensor axes in the manganese(II)–copper(II) case, which is depicted in Figure 4. The spin Hamiltonian parameters obtained are in good agreement with those reported by Kokoszka and co-workers.[10] The magnitudes and orientations of the **g** and hyperfine tensor are quite typical of square-planar and square-pyramidal copper(II) complexes which have a $d_{x^2-y^2}$ ground state.

Theoretical Considerations of the Manganese(II)–Copper(II) Dimer. In principle, the energy levels of a magnetic dimer can be described by a spin Hamiltonian of the form

$$\mathcal{H} = \mathcal{H}_p + \mathcal{H}_s + \mathcal{H}_s'$$

The pairwise interactions between the two metal ions are contained in $\mathcal{H}_p$ while the single ion interactions appropriate for each metal center are included in $\mathcal{H}_s$ and $\mathcal{H}_s'$. The basis set for such a Hamiltonian is constructed by simply taking products of the single ion spin functions $|S, m_s\rangle|S', m_s'\rangle$, where S and S' refer to the total spins of the two ions). For a dimer containing a $S = {}^5/_2$ ion and $S = {}^1/_2$ ion, there will be a total of 12 product functions. Application of the Hamiltonian to the product functions yields a 12 by 12 energy matrix. In general, the eigenvalues and eigenvectors can be found numerically by computer diagonalization of the matrix. The eigenvectors describe the linear combinations of product functions which are eigenfunctions of the complete dimer Hamiltonian, and the eigenvalues correspond to the spin-state energies of the magnetic dimer.

It would be relatively straightforward to write a detailed spin Hamiltonian for the copper(II)–manganese(II) dimer in $[Cu(pyO)Cl_2 \cdot H_2O]_2$. The exchange interaction should have a small anisotropic component superimposed on a relatively large isotropic coupling. With neglect of the hyperfine interactions, the manganese(II) Hamiltonian ($\mathcal{H}_s$) should contain Zeeman and zero-field splitting terms while the copper(II) Hamiltonian ($\mathcal{H}_s'$) should only consist of Zeeman terms. A reliable description of the **g** tensor for the copper(II) ion can be taken from the spectrum of the copper(II)–zinc(II) dimer. Unfortunately, no similar direct indication of the single ion properties of the manganese(II) is available. Although it is safe to assume that the **g** tensor will be nearly isotropic with a g value close to that of a free electron, there is no way of determining the magnitude or orientation of the zero-field splitting tensor. In a low-symmetry environment such as $[Cu(pyO)Cl_2 \cdot H_2O]_2$ the zero-field splitting of a manganese(II) ion should be considerable. Since the fine structure observed in the dimer spectrum arises from both the anisotropic exchange interactions and the manganese(II) zero-field splitting, it is not possible to unambiguously characterize the two interactions. Although this difficulty prevents a full theoretical treatment, considerable insight is gained from a somewhat more simplified approach to the problem.

It seems certain that the exchange coupling is by far the strongest magnetic interaction in the manganese(II)–copper(II) dimer, since the quintet and septet states appear to be separated by at least 150 cm^{-1}. The other magnetic interactions (Zeeman, zero-field splitting, hyperfine, etc.) cannot be greater than a few wavenumbers at most. If the anisotropic interactions are ignored, the exchange coupling should be fairly well described by the familiar scalar product

$$\mathcal{H}_p = JS \cdot S'$$

Since this term undoubtedly dominates the dimer Hamiltonian, the eigenvalues and eigenfunctions of $\mathcal{H}_p$ alone should provide an approximate description of the manganese(II)–copper(II)

Table V. Eigenfunctions[a] of the Quintet ($\Sigma = 2$) and Septet ($\Sigma = 3$) States of the Mn(II)-Cu(II) Dimer

$\Sigma = 2$

$$|2,2\rangle = -\sqrt{1/6}\,|3/2, 1/2\rangle + \sqrt{5/6}\,|5/2, -1/2\rangle$$
$$|2,1\rangle = -\sqrt{1/3}\,|1/2, 1/2\rangle + \sqrt{2/3}\,|3/2, -1/2\rangle$$
$$|2,0\rangle = -\sqrt{1/2}\,|-1/2, 1/2\rangle + \sqrt{1/2}\,|1/2, -1/2\rangle$$
$$|2,-1\rangle = -\sqrt{2/3}\,|-3/2, 1/2\rangle + \sqrt{1/3}\,|-1/2, -1/2\rangle$$
$$|2,-2\rangle = -\sqrt{5/6}\,|-5/2, 1/2\rangle + \sqrt{1/6}\,|-3/2, -1/2\rangle$$

$\Sigma = 3$

$$|3,3\rangle = |5/2, 1/2\rangle$$
$$|3,2\rangle = \sqrt{5/6}\,|3/2, 1/2\rangle + \sqrt{1/6}\,|5/2, -1/2\rangle$$
$$|3,1\rangle = \sqrt{2/3}\,|1/2, 1/2\rangle + \sqrt{1/3}\,|3/2, -1/2\rangle$$
$$|3,0\rangle = \sqrt{1/2}\,|-1/2, 1/2\rangle + \sqrt{1/2}\,|1/2, -1/2\rangle$$
$$|3,-1\rangle = \sqrt{1/3}\,|-3/2, 1/2\rangle + \sqrt{2/3}\,|-1/2, -1/2\rangle$$
$$|3,-2\rangle = \sqrt{1/6}\,|-5/2, 1/2\rangle + \sqrt{5/6}\,|-3/2, -1/2\rangle$$
$$|3,-3\rangle = |-5/2, -1/2\rangle$$

[a] The eigenfunctions are of the form $|\Sigma,m_\Sigma\rangle$ and are linear combinations of the single ion basis functions, $|m_s,m_{s'}\rangle$, where m_s and $m_{s'}$ pertain to Mn(II) and Cu(II), respectively.

system. As expected, fivefold and sevenfold degenerate levels result when the energy matrix constructed from the 12 product functions and $\mathcal{H}_p$ is diagonalized. The two levels are separated by $3J$ and correspond to the previously mentioned quintet and septet states. The eigenfunctions of the quintet and septet are shown in Table V. These functions are designated by the quantum numbers appropriate for a spin quintet ($\Sigma = 2$, $m_\Sigma = \pm 2, \pm 1, 0$) and a spin septet ($\Sigma = 3$, $m_\Sigma = \pm 3, \pm 2, \pm 1, 0$). These quantum numbers refer to the dimer as a whole and are distinct from the single ion quantum numbers. The functions in Table V are quite analogous to those derived by Griffith for a coupled iron(III)–copper(II) system.[12] Within the framework of first-order perturbation theory the eigenfunctions provide a convenient means of relating the g and hyperfine constants of the dimer to the properties of the two individual ions.

As mentioned earlier, the g values of the manganese(II)–copper(II) system are particularly interesting since g_x, g_y, and g_z are lower than the spin-only value. If hyperfine and zero-field splitting interactions are negelected, the Zeeman energies of the dimer states can be computed as simple expectation values. Since the exchange interaction ($\mathcal{H}_p$) is isotropic, the choice of axes is arbitrary. If the axes of quantization are taken to be coincident with the applied magnetic field, the Zeeman energies can be computed as

$$E_z = \langle \Sigma,m_\Sigma|g\beta H\hat{\Sigma}_z|\Sigma,m_\Sigma\rangle = g\beta H m_\Sigma$$

The Zeeman energies can also be computed with use of single ion operators by expressing the eigenfunctions in terms of single ion product functions:

$$g\beta H m_\Sigma = E_z = \beta H\langle \text{product functions}|g_m\hat{S}_z + g_c\hat{S}_z'|\text{product functions}\rangle$$

The operators $\hat{S}$ and S' apply to the spin functions of manganese(II) and copper(II), respectively. Solving for the g value of the dimer, one obtains a relatively simple expression (with $m_\Sigma \neq 0$):

$$g = \frac{1}{m_\Sigma}\sum\langle \text{product functions}|g_m\hat{S}_z + g_c\hat{S}_z'|\text{product functions}\rangle$$

The results shown in Table VI are obtained if g_c is taken from the copper(II)–zinc(II) dimer and g_m is assumed to be equal to the free-electron value, 2.002. The agreement between the

Table VI. Manganese(II)–Copper(II) Dimer g Values[a]

$\Sigma = 2$ state		
calcd	obsd	$\Sigma = 3$ state (calcd)
$g_x = 1.993$	$g_x = 1.991$	$g_x = 2.011$
$g_y = 1.988$	$g_y = 1.986$	$g_y = 2.016$
$g_z = 1.951$	$g_z = 1.952$	$g_z = 2.053$

[a] In the calculations the single ion g values used for copper(II) were those of the copper(II)–zinc(II) dimer given in Table IV. The manganese(II) g tensor was assumed to be isotopic, and the g value was estimated to be 2.002.

observed and calculated values for the quintet state of the copper(II)–manganese(II) dimer is excellent. Although there are no experimental data for the septet state, the calculated g values are shown for comparison. The computations suggest that the g values for the quintet state ($\Sigma = 2$) of any strongly coupled copper(II)–manganese(II) dimer will be less than the free-electron value while those for the septet state ($\Sigma = 3$) will be greater.

The hyperfine constants for the dimer can be computed in a manner similar to that used for the g values. If only diagonal terms are considered, the hyperfine energy can be written as

$$E_{hf} = m_I\langle \Sigma,m_\Sigma|A\hat{\Sigma}_z|\Sigma,m_\Sigma\rangle = m_I m_\Sigma A$$

The hyperfine energy can be expressed in terms of single ion operators:

$$E_{hf} = m_I\langle \text{product functions}|a\hat{S}_z|\text{product functions}\rangle$$

By combining the two expressions, one can solve for both copper and manganese hyperfine constants of the dimer (with $m_\Sigma \neq 0$):

$$A_m = \frac{1}{m_\Sigma}\langle \text{product functions}|a_m\hat{S}_z|\text{product functions}\rangle$$

$$A_c = \frac{1}{m_\Sigma}\langle \text{product functions}|a_c\hat{S}_z'|\text{product functions}\rangle$$

The following relationships are obtained for the quintet and septet states: quintet ($\Sigma = 2$), $A_c = {}^1/_6 a_c$, $A_m = {}^7/_6 a_m$; septet ($\Sigma = 3$), $A_c = {}^1/_6 a_c$, $A_m = {}^5/_6 a_m$. The measured copper hyperfine constants agree quite well with the predictions. The value observed along the z axis of the copper(II)–manganese(II) dimer (0.0023 cm^{-1}) is almost exactly one-sixth of the corresponding value reported for the copper(II)–zinc(II) system (0.0139 cm^{-1}).[10] The result for the manganese hyperfine constants in the quintet state is particularly interesting since the constant for the dimer is predicted to be larger than the single ion constant. Although a direct measurement of a_m in $[Cu(pyO)Cl_2 \cdot H_2O]_2$ is not available, one would predict that a manganese(II) ion coordinated to chloride ions and oxygen-containing ligands would have hyperfine constants in the range of 0.0080–0.0085 cm^{-1}.[13] This estimate is somewhat smaller than the observed dimer constants ($\sim$0.0091 cm^{-1}) which is at least qualitatively consistent with the theoretical prediction.

Comments and Conclusions. As a magnetically coupled system the copper(II)–manganese(II) dimer is a particularly interesting case. It is an example of a magnetic dimer in which the two metal ions contribute different numbers of unpaired electrons. The fact that both metals have nuclear moments makes it possible to obtain a direct indication of the electron distribution in the dimer. The beautifully resolved EPR spectrum provides a considerable amount of detailed information. Although it is not possible to quantitatively interpret every feature, the major spectral characteristics are consistent with relatively simple theoretical considerations. It is hoped

(12) J. S. Griffith, *Mol. Phys.*, **21**, 141 (1971).

(13) B. R. McGarvey, *J. Phys. Chem.*, **71**, 51 (1966).

that the results of this study will provide a useful basis by which the magnetic properties of other mixed metal dimers may be characterized. Although such systems are still relatively rare, efforts to prepare and study heterogeneous magnetic dimers have been made in recent years.[14-18] It appears that mixed dimers may also occur in biological systems. Cytochrome oxidase is reported to contain an antiferromagnetically coupled iron(III)–copper(II) system.[19-21] It is interesting to note that a Fe(III)–Cu(II) dimer is isoelectronic with a Mn(II)–Cu(II) species. Unfortunately, the Fe(III)–Cu(II) system in cytochrome oxidase does not have an observable EPR signal. Presumably, this results from a very large zero-field splitting in the quintet ground state.[12]

Acknowledgment. The authors thank Professor Barry B. Garrett of Florida State University for the use of the E-12 EPR spectrometer and for many helpful discussions. This work was partially supported by National Science Foundation Grant CHE 77-12557.

Registry No. $[Cu(pyO)Cl_2 \cdot H_2O]_2$, 57428-25-8; Mn^{2+}, 16397-91-4.

Supplementary Material Available: A listing of structure factor amplitudes (9 pages). Ordering information is given on any current masthead page.

(14) T. D. Smith and J. D. Pilbrow, *Coord. Chem. Rev.*, **13**, 173 (1974), and references therein.
(15) D. A. Buckingham, M. J. Gunter, and L. N. Mander, *J. Am. Chem. Soc.*, **100**, 2899 (1978).
(16) R. H. Petty and L. J. Wilson, *J. Chem. Soc., Chem. Commun.*, 483 (1978).
(17) C. J. O'Connor, D. P. Freyberg, and E. Sinn, *Inorg. Chem.*, **18**, 1077 (1979).
(18) R. H. Petty, B. R. Welch, L. J. Wilson, L. A. Bottomley, and K. M. Kadish, *J. Am. Chem. Soc.*, in press.
(19) B. F. Van Gelder and H. Beinert, *Biochim. Biophys. Acta*, **189**, 1 (1969).
(20) G. Palmer, G. T. Babcock, and L. E. Vickery, *Proc. Natl. Acad. Sci. U.S.A.*, **73**, 2206 (1976).
(21) M. F. Tweedle, L. F. Wilson, L. Garcia-Iniguez, G. T. Babcock, and G. Palmer, *J. Biol. Chem.*, **253**, 8065 (1978).

Contribution from the Istituto di Chimica Generale, Università di Pisa, 56100 Pisa, Italy, and Istituto di Strutturistica Chimica, Università di Parma, 43100 Parma, Italy

Model Compounds for Copper(I) Sites in Hemocyanins: Synthesis, Structure, and Properties of Copper(I)–Histamine Complexes

MARCO PASQUALI, GIULIANA MARINI, CARLO FLORIANI,* AMELIA GAETANI-MANFREDOTTI, and CARLO GUASTINI

Received December 6, 1979

A methanolic suspension of CuI in the presence of histamine (hm) (hm/CuI > 2) reacts reversibly with carbon monoxide absorbing 1 mol of CO/mol of copper. The absorption of CO produces a slightly green solution from which, by addition of $NaBPh_4$, white crystals of $[Cu_2(hm)_3(CO)_2](BPh_4)_2$ (I) [ν_{CO}(Nujol) 2055 and 2066 cm^{-1}] have been obtained. The X-ray analysis performed on I showed the presence of the dimeric cation $[Cu_2(hm)_3(CO)_2]^{2+}$, with one histamine molecule chelated to each copper atom, one histamine bridging the two metal atoms, and a carbon monoxide molecule completing the pseudotetrahedral geometry around the metal. While the chelating histamine is a 4-imidazole derivative, the bridging one is present in the 5-imidazole form. The reaction between a methanolic suspension of CuCOCl with histamine, carried out at 0 °C, gave a solution from which, by addition of $NaBPh_4$, [Cu(hm)CO]BPh_4 (II) [ν_{CO}(Nujol) 2091 cm^{-1}] was recovered as a crystalline solid. II reacts with an excess of histamine, producing I. A polymeric structure is suggested for II, in which copper(I) is supposed to achieve the tetracoordination through an imidazole ring bridging two copper(I) atoms. Carbonylated solutions from which I and II are obtained react with cyclohexyl isocyanide losing CO and giving, on addition of $NaBPh_4$, the same complex $[Cu(hm)(C_6H_{11}NC)](BPh_4)$ [ν_{CN}(Nujol) 2180 cm^{-1}]. Crystallographic details for $[Cu_2(hm)_3(CO)_2](BPh_4)_2$: space group $P2_1$ (monoclinic), a = 15.901 (2) Å, b = 13.301 (2) Å, c = 14.826 (2) Å, β = 109.30 (1)°; Z = 2. The final R was 9.4% for 2894 observed reflections.

Introduction

The value of a "model compound" depends on the closeness of its physical parameters and chemical properties to those of biological or catalytically active systems. As concerns compounds containing a metal center, these parameters could be (i) the nature of the metal along with its oxidation state and d electron configuration, (ii) the coordination number and coordination geometry around the metal, and (iii) the donor atoms binding the metal active site, along with the nature of the organic molecule bearing these bonding groups. Moreover, the effectiveness of a "model compound" comes out from the degree to which it is able to imitate some of the key functions displayed by the living or catalytic systems.

The presence of copper(I) and copper(II) in some metalloproteins is very well documented.[1-3] While various model compounds have been found for imitating the Cu(II)–protein interaction,[4] very little information is available regarding copper(I) models for Cu(I)–protein interaction.[3,5] One reason for the limited amount of information available is that the oxidation state +1 for copper is mainly stabilized by π-bonding soft donor atoms, i.e., PR_3 and SR_2, which are absent in living systems. Amino groups and imidazolic nitrogens, which bind copper(I) in some metalloproteins, cause, under ordinary reaction conditions, the disproportionation of copper(I) to copper(II) and copper metal.

Rather recently, we found that the use of CuCOCl and CuI, as sources of copper(I) and polydentate amines in a carbon monoxide atmosphere, allows the isolation of mono- and di-

* To whom correspondence should be addressed at the Università di Pisa.

(1) Lontie, A. R.; Witters, R. *Inorg. Biochem.* **1973**, *1*, Chapter 12. Bennett, L. E. *Prog. Inorg. Chem.* **1973**, *18*, 1.
(2) Freedman, T. B.; Loehr, J. S.; Loehr, T. M. *J. Am. Chem. Soc.* **1976**, *98*, 2809. Solvato, B.; Ghiretti-Magaldi, A.; Ghiretti, F. *Biochemistry* **1974**, *13*, 4778.
(3) Osterberg, R. *Coord. Chem. Rev.* **1974**, *12*, 309.
(4) Amundsen, A. R.; Whelan, J.; Bosnich, B. *J. Am. Chem. Soc.* **1977**, *99*, 6730. Addison, A. W.; Carpenter, M.; Lau, L. K.-M.; Wicholas, M. *Inorg. Chem.* **1978**, *17*, 1545. Yokoi, H.; Addison, A. W. *Ibid.* **1977**, *16*, 1341.
(5) Temussi, P. A.; Vitagliano, A. *J. Am. Chem. Soc.* **1975**, *97*, 1572.

0020-1669/80/1319-2525$01.00/0